Four-neutrino mixing solutions of the atmospheric neutrino anomaly

A. Marrone[a]

[a]Dipartimento di Fisica and Sezione INFN di Bari
Via Amendola 173, I-70126 Bari, Italy

Solutions to the atmospheric neutrino anomaly which smoothly interpolate between $\nu_\mu \to \nu_\tau$ and $\nu_\mu \to \nu_s$ oscillations are studied. It is shown that, although the Super-Kamiokande data disfavor the *pure* $\nu_\mu \to \nu_s$ channel, one cannot exclude sizable amplitude for the $\nu_\mu \to \nu_s$ channel *in addition* to $\nu_\mu \to \nu_\tau$ oscillations.

1. Introduction

Four-neutrino (4ν) [1–3] models including a hypothetical sterile state (ν_s) can accommodate the three sources of evidence for ν flavor oscillations coming from atmospheric, solar, and accelerator neutrino experiments. In particular, 4ν spectra with mass eigenstates organized in two doublets (2+2 models) seem to be favored by world neutrino data [4]. Although 2+2 models are often assumed to imply the $\nu_\mu \to \nu_\tau$ or $\nu_\mu \to \nu_s$ channel for solar and atmospheric oscillations, one might have mixed (active+sterile) flavor transitions of the kind [5]

$$\nu_\mu \quad \to \quad \nu_+ \ \text{(atmospheric)} \ , \tag{1}$$

$$\nu_e \quad \to \quad \nu_- \ \text{(solar)} \ , \tag{2}$$

where the states $\nu_\pm$, as discussed in detail in [6], represent linear (orthogonal) combinations of ν_τ and ν_s through a mixing angle ξ. The oscillation modes (1,2) represent generalizations of both modes $\nu_\mu \to \nu_\tau$ and $\nu_\mu \to \nu_s$, to which they reduce for $\sin\xi = 0$ and 1. For generic values of $\sin\xi$, the final states in atmospheric ν_μ and solar ν_e flavor transitions are linear combinations of ν_s and ν_τ, and the coefficients have to be constrained by experiments. In this work, four-neutrino oscillations in the context of 2+2 spectra are studied, for unconstrained values of $\sin\xi = \langle\nu_+|\nu_s\rangle$. It is shown that the state ν_+ (into which ν_μ oscillates) can have a sizable ν_s component. As shown in [6], these results can be reconcilied to the 4ν solutions to the solar neutrino problem [7,8], which are compatible with a large ν_s component of ν_-.

2. Graphical representations

The mixing parameter spaces for atmospheric and solar neutrinos can be represented in triangular plots, embedding unitarity relations of the kind $U_1^2 + U_2^2 + U_3^2 = 1$, [1] holding for the four columns of the mixing matrix U, under suitable approximations [6]. It can be shown that is sufficient to implement just one unitarity relation in one triangle plot for the two mass doublets, the first (ν_3, ν_4) being the atmospheric doublet, the second (ν_1, ν_2) the solar doublet, in our framework. Under the semplifying hypotheses discussed in [6], the ν_e does not take part to the oscillations of atmospheric neutrinos, so that the mixing can be graphically represented in a triangle plot, where the upper, lower left and lower right corner are identified with ν_μ, ν_s, and ν_τ, respectively, and the actual mixing is determined by the position of the ν_4 mass eigenstate in the triangle. The heights projected from a generic point ν_4 inside the triangle onto the lower, right, and left side represent the elements $U_{\mu 4}^2$, U_{s4}^2, and $U_{\tau 4}^2$, respectively. These three matrix elements can be expressed as functions of two mixing angles (ψ , ξ). The square mass difference m^2 between the atmospheric doublet (ν_3, ν_4) completes the parametrization. When ν_4 coincides with one of the corners no oscillation occur. Generic points inside the triangle describe mixed (active+sterile) atmospheric neutrino oscillations, smoothly interpolating from pure $\nu_\mu \to s$ to pure $\nu_\mu \to \nu_\tau$.

[1] Triangle plots have been already introduced and discussed in detail in the context of 3ν mixing, see [10].

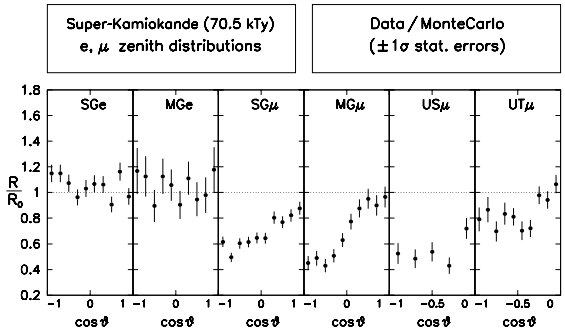

Figure 1. Super-Kamiokande data on zenith distributions of lepton events induced by atmospheric neutrinos.

3. Results of the atmospheric ν analysis

The most recent 70.5 kTy Super-Kamiokande data used in our analysis [9] are shown in Figure 1. The statistical χ^2 analysis is similar to that of [10]. Figures 2 and 3 show the results of our analysis in the atmospheric triangle plot. The first three columns of triangles refer to the separate fits to sub-GeV electrons and muons (10+10 bins), multi-GeV electrons and muons (10+10 bins), and upward stopping and through-going muons (5+10 bins), while the fourth column refers to the total SK data sample (55 bins). For each column, we find the minimum χ^2 from the fit to the corresponding data sample, and then present sections of the allowed volume at fixed values of m^2 for $\Delta\chi^2 = 6.25$ (90% C.L., solid lines) and $\Delta\chi^2 = 11.36$ (99% C.L., dotted lines). The low-energy SG data are basically insensitive to s^2_ξ, since they are consistent both with $\nu_\mu \to \nu_\tau$ oscillations (left side) and with $\nu_\mu \to \nu_s$ oscillations (right side), as well as with any intermediate combination of the two oscillation channels. High-energy upgoing muon data are instead much more sensitive to the ν_s component through matter effects, which increase both with energy and with s^2_ξ, and tend to suppress the muon deficit. Large matter effects appear to be disfavored by the upgoing muon data, the rightmost part of the triangle being excluded at

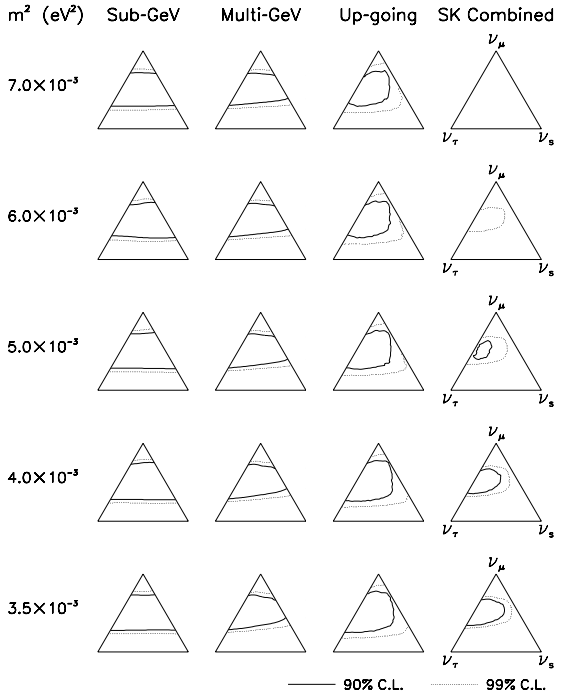

Figure 2. Results of the global fit to atmospheric neutrino data in the triangular plots, for decresing m^2 values.

90% C.L. The multi-GeV data cover an intermediate energy range and are not as constraining as the upgoing muons. However, they show a tendency to disfavor a large sterile component, that is strengthened in the global combination of data (fourth column), leading to the upper bound

$$s^2_\xi \lesssim 0.67 \text{ (90\% C.L.)} , \qquad (3)$$

which disfavors pure or quasi-pure $\nu_\mu \to \nu_s$ oscillations. From Figs. 2 and 3 we derive that pure $\nu_\mu \to \nu_s$ oscillations are excluded at $> 99\%$ C.L., in agreement whith SK results [11]. However, the bound (3) still allows intermediate cases of oscillations with a sizable ν_s component. For instance, one cannot exclude that the sterile neutrino channel may have the same amplitude as the active one ($s^2_\xi = 0.5$), or may even be dominant. Furthermore, for m^2 in its upper range, a subdominant ν_s component actually helps in the global fit

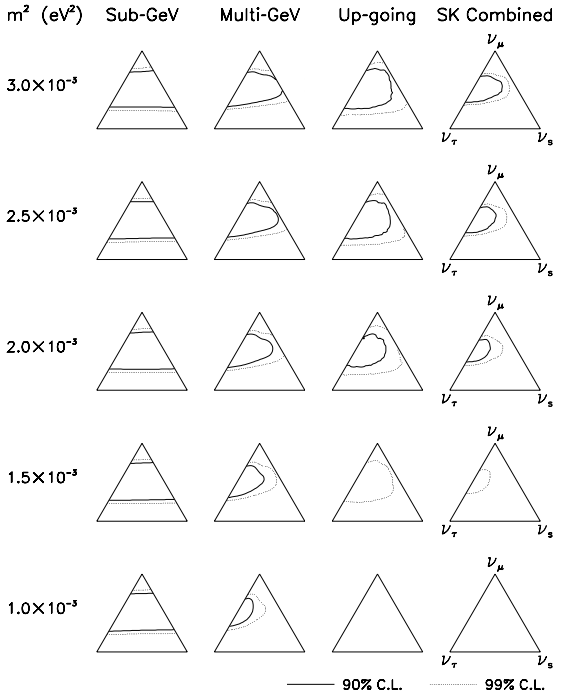

Figure 3. As in Fig. 2, for lower m^2 values.

to SK data, leading to a 90% C.L. allowed region which does not touch the left side of the triangle (pure $\nu_\mu \to \nu_\tau$ channel).

Figures 2 and 3 also provide bounds on the other mixing parameter s^2_ψ, which governs the relative amount of ν_μ and ν_+ on the atmospheric neutrino states ν_3 and ν_4 and thus the overall amplitude of $\nu_\mu \to \nu_+$ oscillations. The following limit can be derived

$$s^2_\psi \simeq 0.51 \pm 0.17 \text{ (90\% C.L.)} , \qquad (4)$$

which favors $\nu_\mu \to \nu_+$ oscillations with nearly maximal amplitude, as expected from the observation of nearly maximal average suppression ($\sim 50\%$) of upgoing MG muons. Therefore, on the basis of present SK data on the zenith distributions of leptons induced by atmospheric neutrinos, pure $\nu_\mu \to \nu_s$ oscillations are strongly disfavored, but one cannot exclude mixed active-sterile $\nu_\mu \to \nu_+$ oscillations, provided that the partial amplitude of the sterile channel is $\lesssim 67\%$.

4. Summary and conclusions

In the context of 2+2 neutrino models, the SK atmospheric data have been studied, assuming the coexistence of both $\nu_\mu \to \nu_\tau$ and $\nu_\mu \to \nu_s$ oscillations, with a smooth interpolation between such two subcases. It has been shown that, although the data disfavor oscillations in the pure $\nu_\mu \to \nu_s$ channel, one cannot exclude their presence *in addition* to $\nu_\mu \to \nu_\tau$ oscillations. High energy muon data appear to be crucial to determine the relative amplitude of the active and sterile oscillation channels for atmospheric neutrinos.

REFERENCES

1. S.M. Bilenky, C. Giunti, and W. Grimus, Prog. Part. Nucl. Phys. **43**, 1 (2000).
2. D. Dooling, C. Giunti, K. Kang, and C.W. Kim, Phys. Rev. D **61**, 073011 (2000).
3. V. Barger and K. Whisnant, hep-ph/0006235, in *Current Aspects of Neutrino Physics*, ed. by D. Caldwell (Springer-Verlag, Hamburg, 2000).
4. S.M. Bilenky, C. Giunti, and W. Grimus, Proceedings of *Neutrino '96*, Helsinki, June 1996, edited by K. Enqvist *et al.* (World Scientific, Singapore, 1997), p.174, hep-ph/9609343; V. Barger, S. Pakvasa, T.J. Weiler, and K. Whisnant, Phys. Rev. D **58**, 093016 (1998).
5. G.L. Fogli, E. Lisi, and A. Marrone, in *Neutrino 2000*, 19th International Conference on Neutrino Physics and Astrophysics (Sudbury, Canada, 2000), to appear; transparencies available at the site http://nu2000.sno.laurentian.ca.
6. G.L. Fogli, E. Lisi, and A. Marrone, hep-ph/0009299, accepted by Phys. Rev. D.
7. C. Giunti, M.C. Gonzalez-Garcia, and C. Peña-Garay, Phys. Rev. D **62**, 013005 (2000).
8. M.C. Gonzalez-Garcia and C. Peña-Garay, hep-ph/0009041.
9. H. Sobel for the Super-Kamiokande Collaboration, in *Neutrino 2000* [5].
10. G.L. Fogli, E. Lisi, A. Marrone, and G. Scioscia, Phys. Rev. D **59**, 033001 (1999).
11. Super-Kamiokande Collaboration, S. Fukuda *et al.*, Phys. Rev. Lett. **85**, 3999 (2000).

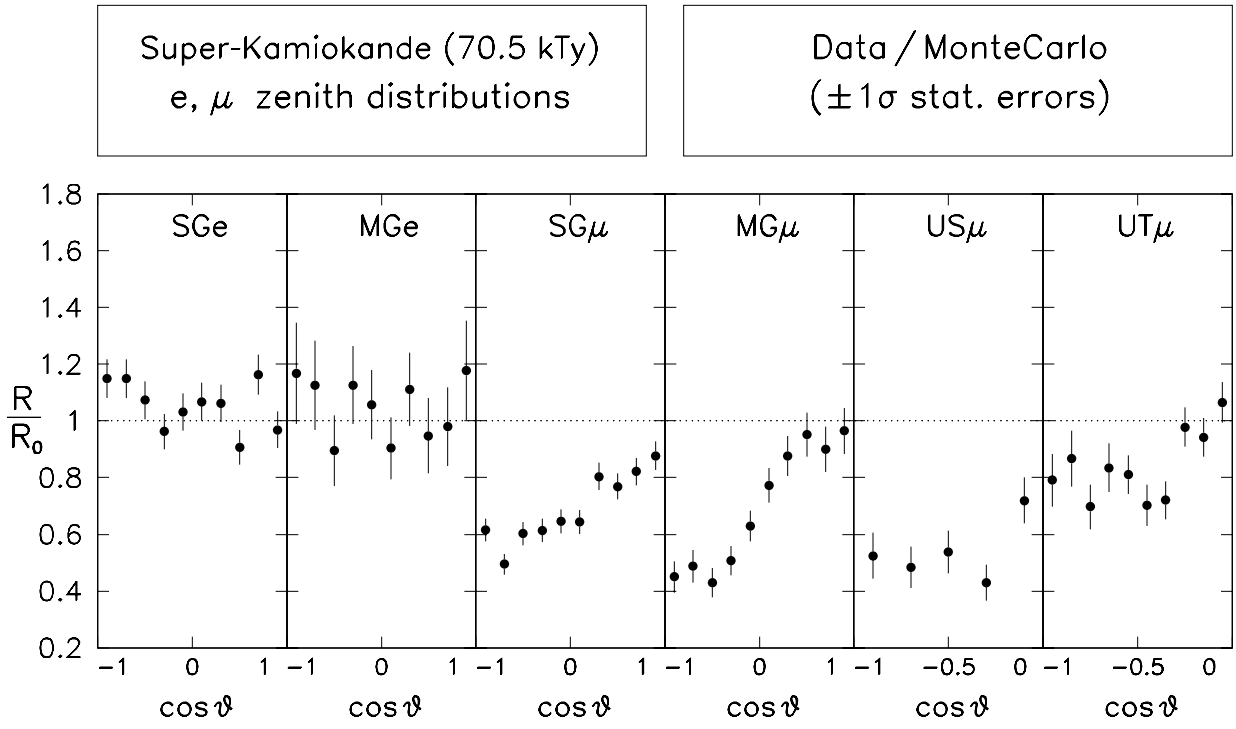
Super-Kamiokande (70.5 kTy)
e, μ zenith distributions
Data / MonteCarlo
(±1σ stat. errors)
SGe
MGe
SGμ
MGμ
USμ
UTμ
R/R0
cos ϑ

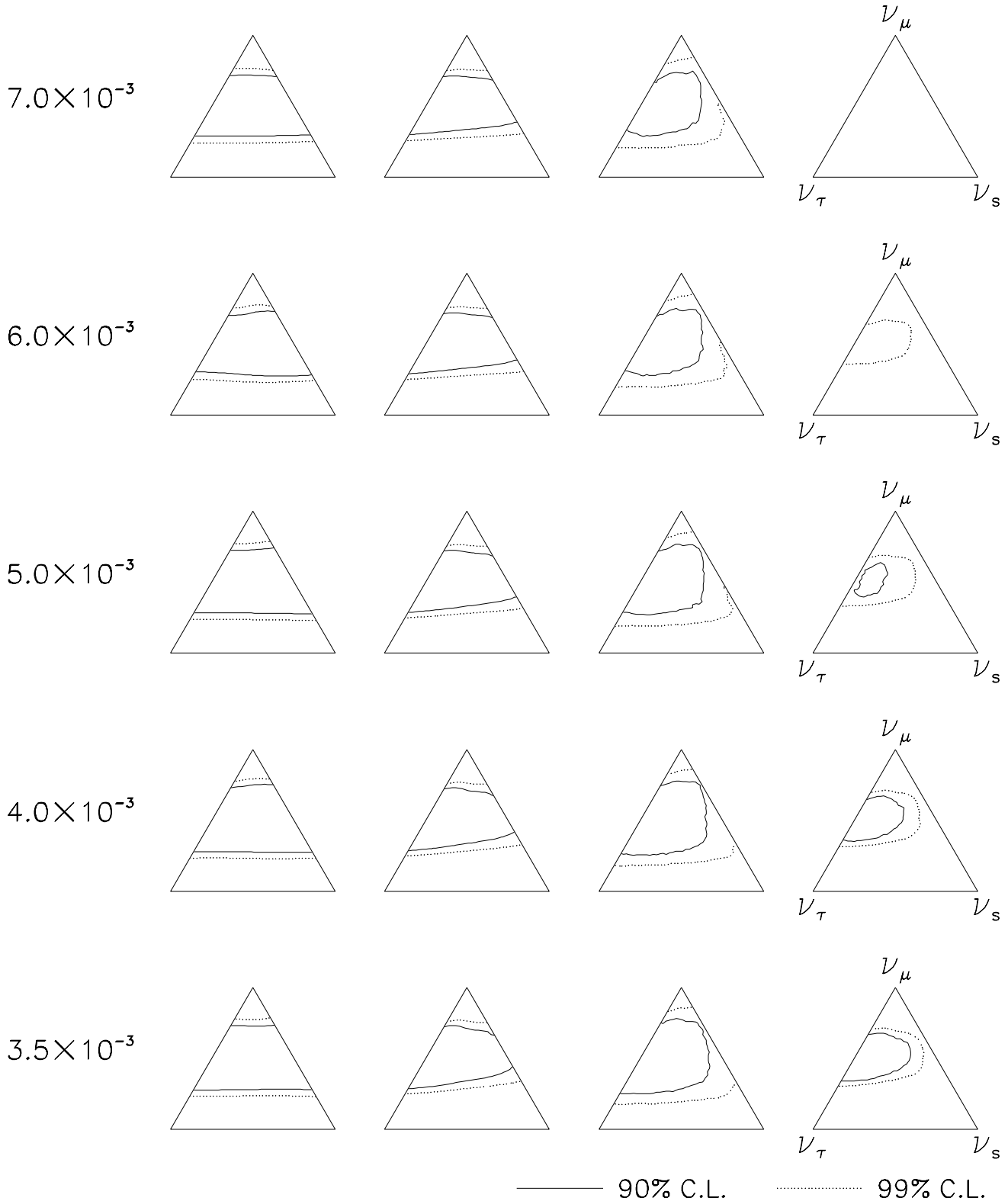
m² (eV²)
Sub-GeV
Multi-GeV
Up-going
SK Combined
7.0×10⁻³
6.0×10⁻³
5.0×10⁻³
4.0×10⁻³
3.5×10⁻³
ν_μ
ν_τ
ν_s
90% C.L.
99% C.L.

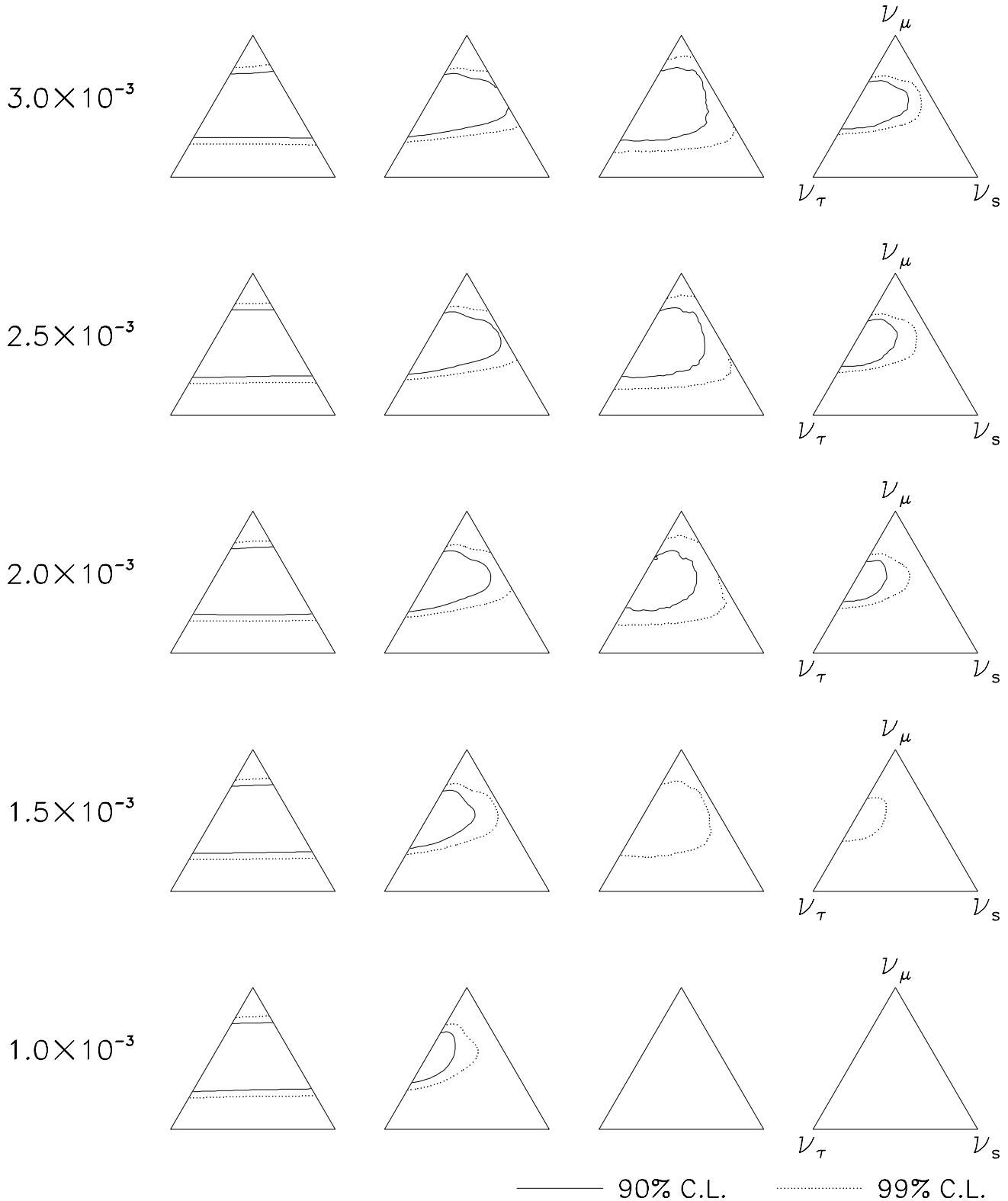
m^2 (eV^2)
Sub-GeV
Multi-GeV
Up-going
SK Combined
3.0×10^{-3}
2.5×10^{-3}
2.0×10^{-3}
1.5×10^{-3}
1.0×10^{-3}
ν_μ
ν_τ
ν_s
90% C.L.
99% C.L.